Accurate Coarse-Grained Modeling of Red Blood Cells

Igor V. Pivkin* and George Em Karniadakis+

Division of Applied Mathematics, Brown University, Providence, Rhode Island 02912, USA

(Received 6 September 2007; published 12 September 2008)

We develop a systematic coarse-graining procedure for modeling red blood cells (RBCs) using arguments based on mean-field theory. The three-dimensional RBC membrane model takes into account the bending energy, in-plane shear energy, and constraints of fixed surface area and fixed enclosed volume. The coarse-graining procedure is general, it can be used for arbitrary level of coarse-graining and does not employ any fitting parameters. The sensitivity of the coarse-grained model is investigated and its behavior is validated against available experimental data and in dissipative particle dynamics (DPD) simulations of RBCs in capillary and shear flows.

DOI: 10.1103/PhysRevLett.101.118105 PACS numbers: 87.16.D−, 83.50.−v, 83.10.Rs

The human red blood cell (RBC) has a biconcave shape with the diameter of about 8 μm. The RBC membrane is composed of a lipid bilayer and an attached cytoskeleton. The cytoskeleton consists primarily of spectrin proteins, which form the network by linking short actin filaments, resulting in junction complexes. The importance of understanding the mechanical properties of RBCs motivated a number of experimental [1–5] and theoretical studies [6–9]. Continuum- and molecular-based numerical models [10–19] have also been developed and applied to RBC simulations. The level of detail of the RBC membrane description in these studies varies. The model developed in Ref. [12] and later extended in Ref. [13] describes the RBC spectrin network with resolution down to individual junction complexes but it involves about 3×10^4 degrees of freedom (DOF). It was successfully validated against experimental data of the mechanical response of an individual cell, however application of the model in flow simulations requires prohibitively expensive computations. In this Letter, we develop a systematic coarse-graining procedure, which allows us to reduce the number of DOFs in the RBC model by 2 orders of magnitude. Together with a coarse-grained flow model, such as the dissipative particle dynamics (DPD) method, it could lead to efficient simulations of RBCs in microcirculation.

The membrane model consists of a collection of points $\{\mathbf{x}_n, n \in 1 \ldots N\}$, which are the vertices of the RBC surface triangulation. The area of triangle $\alpha \in 1 \ldots \Pi$ formed by vertices (l, m, n) is given by $A_\alpha = |(\mathbf{x}_m - \mathbf{x}_l) \times (\mathbf{x}_n - \mathbf{x}_l)|/2$. The length of the link $i \in 1 \ldots S$ connecting vertices m and n in the triangulation is given by $L_i = |\mathbf{x}_m - \mathbf{x}_n|$. The Helmholtz free energy of the system is

$$F(\{\mathbf{x}_n\}) = F_{\text{in-plane}} + F_{\text{bending}} + F_{\text{volume}} + F_{\text{area}}. \quad (1)$$

The in-plane free energy term

$$F_{\text{in-plane}} = \sum_{i \in \text{links}} V_{\text{WLC}}(L_i) + \sum_{\alpha \in \text{triangles}} C/A_\alpha, \quad (2)$$

includes the wormlike chain (WLC) potential for individual links

$$V_{\text{WLC}}(L) = \frac{k_B T L_{\max}}{4p} \frac{3x^2 - 2x^3}{1 - x}, \quad (3)$$

where $x = L/L_{\max} \in (0, 1)$, $L_{\max}$ is the maximum length of the links and p is the persistence length; the parameter C in the hydrostatic elastic energy term is set as described in Ref. [12], i.e.,

$$C = \frac{3\sqrt{3} k_B T L_{\max}^3 x_0^4}{64p} \frac{4x_0^2 - 9x_0 + 6}{(1 - x_0)^2}. \quad (4)$$

The bending energy [20] is given by

$$F_{\text{bending}} = \sum_{\text{adjacent}\alpha,\beta\text{pair}} k_{\text{bend}}[1 - \cos(\theta_{\alpha\beta} - \theta_0)], \quad (5)$$

where k_{bend} is the average bending modulus [21], while θ_0 and $\theta_{\alpha\beta}$ are the spontaneous and the instantaneous angles between two adjacent triangles, respectively. Well known expressions for the total volume and area terms in the Eq. (1) are used here [22]. The forces are obtained from $\mathbf{f}_n = -\partial F(\{\mathbf{x}_n\})/\partial \mathbf{x}_n$, while the evolution of the velocity and coordinates of the typical point $n \in 1 \ldots N$ is described by Newton's equations of motion

$$\frac{d\mathbf{x}_n}{dt} = \mathbf{v}_n; \qquad \frac{d\mathbf{v}_n}{dt} = \mathbf{f}_n + \mathbf{f}_n^{\text{ext}}, \quad (6)$$

where $\mathbf{v}_n$ is velocity and $\mathbf{f}_n^{\text{ext}}$ is the external force applied on the point.

The model used in Ref. [13] consisted of $N = 23\,867$ points, each representing a junction complex in the RBC spectrin network. The average length of links L_0 was 75 nm. The maximum extension length $L_{\max}$ was taken to be $3.17L_0$ and the persistence length was $p = 7.5$ nm. The average bending modulus was $k_{\text{bend}} = 200k_BT$ and the spontaneous angle $\theta_0 = 1°$. The model produced results in good agreement with the optical tweezers experiment data [13]. (We will refer to this model as "fine" model and mark its parameters with superscript "f" later in the text.)

In a series of experiments [2] it was shown that RBCs subject to a transient shear flow after relaxation recover a biconcave shape in which the rim of the cell is always formed by the same part of the membrane. These results suggest that there is an elastic energy stored in the membrane components that has a minimum when the RBC is in discocyte state and that the local components of the membrane are not strained in the biconcave resting shape [4,19]. Therefore, the material reference state for the in-plane elastic energy of the model is chosen to be a biconcave shape. The average shape of the unstressed biconcave RBC measured experimentally is given by a set of points with coordinates (x, y, z) in 3D space satisfying the following equation

$$y = R\sqrt{1 - \frac{x^2 + z^2}{R^2}}\left[c_0 + c_1\frac{x^2 + z^2}{R^2} + c_2\frac{(x^2 + z^2)^2}{R^4}\right], \quad (7)$$

where $(R, c_0, c_1, c_2) = (3.91\ \mu\text{m}, 0.013\,580\,5, 1.001\,279, -0.561\,381)$ [23]. We used the following procedure to obtain the initial biconcave shape: First, the points are uniformly distributed over the analytic shape (7) and used as vertices for the surface triangulation. Next, the motion of the points is restricted to the biconcave shape, while their positions are updated due to the relaxation of the free energy of the model. During this process, the links are swapped to ensure that for each pair of adjacent triangles the edge between the triangles is the shorter diagonal connecting pairs of opposite vertices. The final state is obtained after sufficiently long-time equilibration.

We develop a coarse-grained model by using a smaller number of points ($N < 23\,867$) to represent the RBC. The equilibrium length of the links depends on the number of particles used. The simple approximation, based on a geometric argument of average increase of membrane area per point,

$$L_0^c = L_0^f\sqrt{\frac{N^f}{N^c}} \quad (8)$$

used here gave good results, where N^f and N^c are number of points in the fine and coarse-grained models, respectively, and L_0^c is the equilibrium length of the links in the coarse-grained model. The average angle between the pairs of adjacent triangles increases as we coarse-grain the model. Therefore, using a similar geometric argument, we adjust the spontaneous angle as

$$\theta_0^c = \theta_0^f\frac{L_0^c}{L_0^f}. \quad (9)$$

To set the parameters in the in-plane shear energy equation we use a mean-field argument [12,24]. The mean-field approximation is analytic and the expressions for the parameters of the network can be derived as in Ref. [25]. For the shear modulus of the cell membrane we obtain

$$\mu_0 = \frac{\sqrt{3}k_BT}{4pL_{\max}x_0}\left(\frac{3}{4(1-x_0)^2} - \frac{3}{4} + 4x_0 + \frac{x_0}{2(1-x_0)^3}\right), \quad (10)$$

TABLE I. Effective parameters of the model (SI units) at different levels of coarse graining at temperature $T = 300$ K. Parameters are described in the text.

N	L_0	$L_{\max}$	p	C	θ_0
23 867	7.50×10^{-8}	$3.17L_0$	7.50×10^{-9}	1.81×10^{-34}	1.00°
5000	1.63×10^{-7}	$3.17L_0$	3.43×10^{-9}	4.13×10^{-33}	2.18°
500	5.18×10^{-7}	$3.17L_0$	1.08×10^{-9}	4.13×10^{-31}	6.90°
100	1.15×10^{-6}	$3.17L_0$	4.85×10^{-10}	1.03×10^{-29}	15.44°

and for the elastic area compression modulus

$$K = \frac{\sqrt{3}k_BT}{4pL_{\max}(1-x_0)^2} \times \left(\frac{3}{2}(6 - 9x_0 + 4x_0^2) + \frac{1 + 2(1-x_0)^3}{1-x_0}\right). \quad (11)$$

We notice that for a fixed value of $x_0 = L_0/L_{\max}$, the shear and elastic area compression moduli [26] of the coarse-grained membrane are equal to the original moduli if the persistence length is adjusted as

$$p^c = p^f\frac{L_0^f}{L_0^c}. \quad (12)$$

The system of Eqs. (4), (8), (9), and (12) provides us with a complete set of parameters for the model at *arbitrary* level of coarse-graining, as long as the number of points is sufficient to describe the deformation of the cell adequately. The parameters of the model for different values of coarse graining used later in the text are listed in Table I.

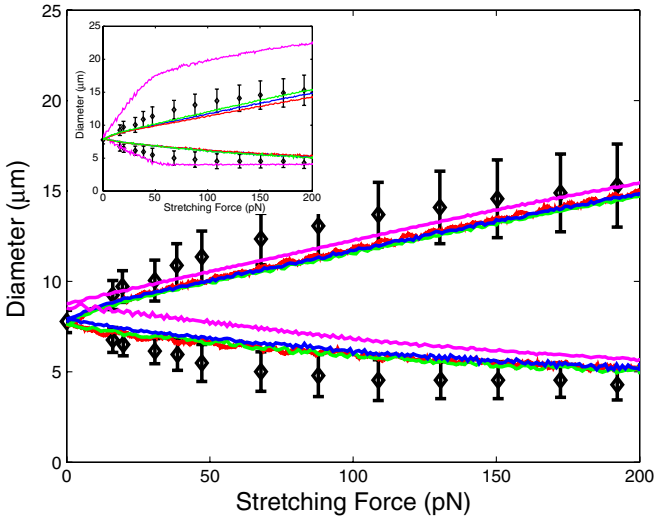

FIG. 1 (color online). Axial and transverse diameters of the RBC versus stretching force. The optical tweezers experimental data from [3] shown with symbols. The simulation results at different levels of coarse-graining are shown with lines. Blue line: $N = 23867$, red line: $N = 5000$, green line $N = 500$ and magenta: $N = 100$. Inset: Persistent length sensitivity study for $N = 500$. Blue line: p is specified according to Eq. (12). Magenta line: $p = 7.5$ nm. Green and red lines: p is set 10% above or below the value given by Eq. (12), respectively.

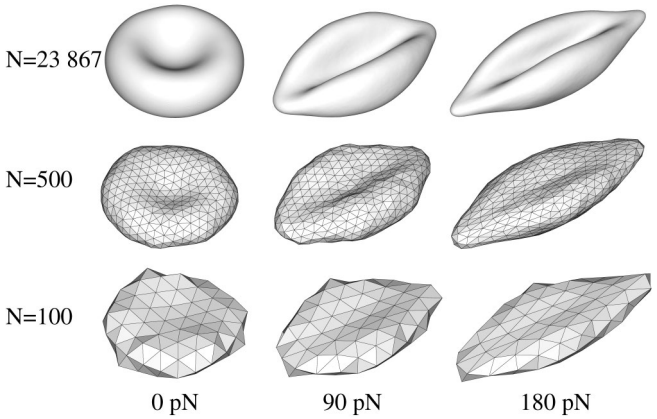

FIG. 2. RBC shape evolution at different stretch forces (0, 90, and 180 pN) predicted by the model at different levels of coarse-graining. Upper row: $N = 23\,867$ (surface triangulation not shown), middle row: $N = 500$, lower row: $N = 100$.

To verify the coarse-graining procedure, we first perform a set of cell stretching experiments at different levels of coarse graining. The data used to investigate the performance of the model was taken from the optical tweezers experiments [3]. Initially, the model is at rest with the large diameters of the model located in the xz plane. We find the 5% of points with the largest x coordinates. During the simulations, we apply the time-dependent force $\mathbf{f}_n^{\text{ext}} = \mathbf{f}_{\text{total}}^{\text{ext}}(t)/(0.05N)$ to each of these points. Similarly, a force $\mathbf{f}_n^{\text{ext}} = -\mathbf{f}_{\text{total}}^{\text{ext}}(t)/(0.05N)$ is applied to the 5% of points with the smallest x-coordinates at rest. The axial and transverse diameters are computed as $|\max_{n\in 1..N} x_n - \min_{n\in 1..N} x_n|$ and $2 \times \max_{n\in 1..N} \sqrt{y_n^2 + z_n^2}$, respectively. The results of the simulations are shown in Fig. 1 and are in good agreement with experimental data. For $N = 100$, the model gives a very crude approximation of the RBC surface as shown in Fig. 2. We start to observe deviations of the axial and transverse diameters, which become more pronounced as we coarse-grain the model further ($N = 50$, not shown here). Therefore, we conclude that $N > 100$ is required to represent the deformation of the RBC accurately. To assess the *sensitivity* of the results for the coarse-grained model on the parameters we perform additional simulations, where we use the fine model persistence length (i.e., set $p = 7.5$ nm) or prescribe it 10% above or below the value given by Eq. (12). In the later cases we observe linear deviations in the axial and transverse diameters, while in the former case the model produces erroneous results as shown in the insert in Fig. 1 for $N = 500$.

Next, we apply the coarse-grained model to simulate the motion of the RBC in a microchannel using dissipative particle dynamics (DPD), a mesoscopic method which describes *clusters* of molecules moving together in a Lagrangian fashion subject to soft quadratic potentials; see Refs. [27,28]. The RBC is modeled as a collection of N DPD particles. This model is immersed in DPD fluid. The RBC particles interact with the fluid particles through DPD potentials [28] and the temperature of the system is controlled through the DPD thermostat [28]. The deformation and motion of the RBC are computed based on Eq. (6), in which the external force, $\mathbf{f}_n^{\text{ext}}$, comes from the interaction with the surrounding DPD fluid. The flow domain is a tube, 45 μm in length and 10 μm in diameter [29]. In the capillaries of this diameter, the blood velocity is typically about 1 mm/s [30]. The no-slip condition at the fluid-solid interface is achieved by using adaptive control [31] with uniform density profile prescribed in the near-wall region. Initially, the fluid is at rest and the RBC is placed in the middle of the channel. We apply a body force in the axial direction to drive the flow in the tube. The RBC deforms under the flow conditions and after some transition period assumes the parachute type shape shown in Fig. 3, which is commonly observed in experiments [5]. After the body force is *turned off* the flow slows down and eventually the DPD fluid returns to rest, while the RBC recovers its equilibrium biconcave shape. The results of Fig. 3 are shown for $N = 500$, but similar results are obtained for more refined models (e.g., $N = 5000$) if the parameters are scaled appropriately using Eqs. (4), (8), (9), and (12).

Using DPD, we have also simulated the motion of the RBC in *shear flow*. An unsteady tumbling solidlike motion was observed, while at high shear stress a tank-treading motion, characterized by membrane rotation about the internal fluid, was predicted in agreement with [19], see Fig. 4. Swinging motion in which the RBC oscillated twice about the mean inclination angle in each tank-treading cycle [4,19] was also observed. The motion in the intermittent region [4,19] had characteristics of both tank treading and tumbling, however it was difficult to separate

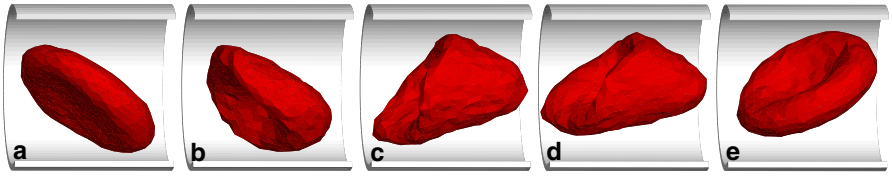

FIG. 3 (color online). Successive snapshots of deformation of the coarse-grained model ($N = 500$) from the DPD simulations of the RBC flow in a microchannel. From left to right: (a) The model is placed in the channel with the fluid at rest. (b),(c) The deformation of the model 0.008 and 0.016 seconds after the body force driving the flow is applied. (d) The shape of the model at steady flow. (e) The model recovers its equilibrium biconcave shape 0.2 seconds [32] after the body force is turned off. (Only a portion on the microchannel is shown for clarity.)

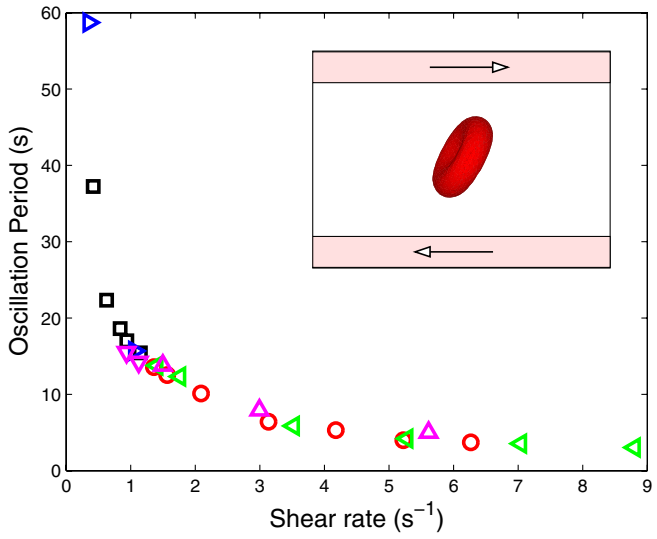

FIG. 4 (color online). Transition from tumbling (□, ▷, ▽) to tank treading (○, ◁, △) of coarse-grained ($N = 500$, 1000, 5000, respectively) RBC model in shear flow in DPD simulations.

clearly these two regimes. The shear stress dependent transition of motion can be explained on the basis of the elastic energy storage in the RBC membrane [4,19].

In this Letter we have developed a coarse-grained model of RBC and applied it in DPD flow simulations. The model can be used with other particle based methods, such as smoothed particle hydrodynamics (SPH) or lattice Boltzmann method (LBM), as well as continuum-based methods. For RBC suspensions, appropriate interaction models should be employed.

This work was supported by the NSF/IMAG, and computations were performed on the IBM Blue Gene at SDSC (an NSF supercomputing center).

*piv@dam.brown.edu
+gk@dam.brown.edu

[1] R. P. Rand and A. C. Burton, Biophys. J. **4**, 115 (1964).
[2] T. M. Fischer, Biophys. J.**86**, 3304 (2004).
[3] J. P. Mills, L. Qie, M. Dao, C. T. Lim, and S. Suresh, Mech. Chem. Biosys. **1**, 169 (2004).
[4] M. Abkarian, M. Faivre, and A. Viallat, Phys. Rev. Lett. **98**, 188302 (2007).
[5] G. Tomaiuolo, V. Preziosi, M. Simeone, S. Guido, R. Ciancia, V. Martinelli, C. Rinaldi, and B. Rotoli, Ann Ist Super Sanita **43**, 186 (2007).
[6] P. B. Canham, J. Theor. Biol. **26**, 61 (1970).
[7] W. Helfrich, Z Naturforsch C **28**, 639 (1973).
[8] U. Seifert, K. Berndl, and R. Lipowsky, Phys. Rev. A **44**, 1182 (1991).
[9] C. Misbah, Phys. Rev. Lett. **96**, 028104 (2006).
[10] D. H. Boal, U. Seifert, and A. Zilker, Phys. Rev. Lett. **69**, 3405 (1992).
[11] J. C. Hansen, R. Skalak, S. Chien, and A. Hoger, Biophys. J. **72**, 2369 (1997).
[12] D. E. Discher, D. H. Boal, and S. K. Boey, Biophys. J. **75**, 1584 (1998).
[13] J. Li, M. Dao, C. T. Lim, and S. Suresh, Biophys. J. **88**, 3707 (2005).
[14] Y. Liu and W. K. Liu, J. Comput. Phys. **220**, 139 (2006).
[15] C. D. Eggleton and A. S. Popel, Phys. Fluids **10**, 1834 (1998).
[16] H. Noguchi and G. Gompper, Proc. Natl. Acad. Sci. U.S.A. **102**, 14159 (2005).
[17] C. Pozrikidis, Annu. Biomed. Eng. **33**, 165 (2005).
[18] J. Li, G. Lykotrafitis, M. Dao, and S. Suresh, Proc. Natl. Acad. Sci. U.S.A. **104**, 4937 (2007).
[19] J. M. Skotheim and T. W. Secomb, Phys. Rev. Lett. **98**, 078301 (2007).
[20] A more accurate discretization of the bending energy includes weighting of the contribution from the pair of triangles by their area product and normalized by the mean product overall such triangle pairs [13]. No significant difference was found in simulations using weighted discretization.
[21] D. H. Boal and M. Rao, Phys. Rev. A **46**, 3037 (1992).
[22] The volume and surface area energy terms are defined as $F_{\text{volume}} = [k_{\text{volume}}(\Omega_{\text{total}} - \Omega_{\text{total}}^{\text{desired}})^2 k_B T]/[2L_0^3 \Omega_{\text{total}}^{\text{desired}}]$, $F_{\text{area}} = [k_{\text{area}}(A_{\text{total}} - A_{\text{total}}^{\text{desired}})^2 k_B T]/[2L_0^2 A_{\text{total}}^{\text{desired}}]$. See, for example, Ref. [13] for details. To keep the total volume and surface area variations within few percent we set k_{volume} and k_{area} equal to 6000 in all simulations.
[23] E. A. Evans and R. Skalak, *Mechanics and Thermodynamics of Biomembranes* (CRC Press, Boca Raton, Fla., 1980).
[24] D. H. Boal, U. Seifert, and J. C. Shillcock, Phys. Rev. E **48**, 4274 (1993).
[25] M. Dao, J. Li, and S. Suresh, Mat. Sci. Eng. C-BioS **26**, 1232 (2006).
[26] Young's modulus, E, and Poisson's ratio, ν, are functions of the linear elastic area compression modulus, K and shear modulus, μ_0; see Ref. [25].
[27] P. J. Hoogerburgge and J. M. Koelman, Europhys. Lett. **19**, 155 (1992).
[28] R. D. Groot and P. B. Warren, J. Chem. Phys. **107**, 4423 (1997).
[29] We follow the notation in Ref. [28] with the DPD parameters $\rho = 3$, $a = 75/\rho k_B T$, $\sigma = 3$, $\gamma = 45$, $r_c = 1$. We set the unit of length, r_c, to be equal to 1 μm and the velocity of RBC at steady flow to be 1 mm/s. The RBC and channel radii are 3.91 and 5.0 μm, respectively.
[30] A. C. Guyton, *Textbook of Medical Physiology* (W.B. Saunders Company, Philadelphia, PA, 1991).
[31] I. V. Pivkin and G. E. Karniadakis, Phys. Rev. Lett. **96**, 206001 (2006).
[32] M. Dao, C. T. Lim, and S. Suresh, J. Mech. Phys. Solids **51**, 2259 (2003).